PHYSICAL REVIEW E **78**, 060902(R) (2008)

Population mixture model for nonlinear telomere dynamics

Shalev Itzkovitz,[1,*] Liran I. Shlush,[2,*] Dan Gluck,[3] and Karl Skorecki[2]
[1]*Department of Computer Science and Applied Mathematics, Weizmann Institute of Science, Rehovot, Israel*
[2]*Rappaport Faculty of Medicine and Research Institute, Technion and Rambam Medical Center, Haifa, Israel*
[3]*Department of Molecular Genetics, Weizmann Institute of Science, Rehovot, Israel*
(Received 27 July 2008; published 23 December 2008)

Telomeres are DNA repeats protecting chromosomal ends which shorten with each cell division, eventually leading to cessation of cell growth. We present a population mixture model that predicts an exponential decrease in telomere length with time. We analytically solve the dynamics of the telomere length distribution. The model provides an excellent fit to available telomere data and accounts for the previously unexplained observation of telomere elongation following stress and bone marrow transplantation, thereby providing insight into the nature of the telomere clock.

DOI: 10.1103/PhysRevE.78.060902 PACS number(s): 87.18.Vf

Telomeres are regions of repetitive DNA sequences at the ends of linear chromosomes that protect them from attrition. The telomere length decreases with each cell division in most cells, eventually signaling cells to stop growing (a state termed "cellular senescence" [1]). Thus telomeres serve as internal clocks for cells, effectively counting the number of cell divisions. The nature of telomere length dynamics is relevant to understanding tissue maintenance, aging, and cancer [2].

In tissue culture, the telomere length of cells decreases linearly with the number of cell divisions [1,3,4]. However, *in vivo*, the dynamics of the average telomere length is more complex—a rapid drop in the first few years of life is followed by a more gradual decrease [5–10]. Most existing mathematical models of *in vivo* telomere shortening either do not account for this nonlinearity [11] or attribute it to a changing cell division rate of stem cells [8–10], experimental evidence for which is still lacking [12].

Here we show that telomere nonlinear dynamics can arise if cell populations are not homogeneous, but rather consist of a mixture of pools with different dynamical properties. Our model posits two pools of cells—a repopulating pool of C_r cells, which consists of either stem cells or a subpopulation of stem cells, and a derived pool of $C \gg C_r$ cells (Fig. 1). A similar model has been used to describe telomere length differences between naive and memory T cells [13]. We assume that the telomere length in the repopulating pool remains constant throughout time, either as a result of infrequent divisions or through the activity of mechanisms which preserve telomere length (e.g., telomerase activity [14–16]). In contrast, the telomere length in cells of the derived pool reduces by a constant fraction of Δ base pairs per cell division.

At any time point a derived cell has a constant rate M of dividing and a constant rate D of dying, which is independent of the cell's telomere length [11]. In addition, at each time point with a rate $M_r \ll M$ repopulating cells undergo asymmetric divisions, giving rise to one daughter cell which stays in the repopulating pool and another which undergoes rapid clonal expansion and whose progeny transfer to the derived pool [2] (Fig. 1). Thus there is a constant influx of $\alpha = f M_r C_r$ cells per time into the derived pool, where f is the clonal expansion factor [13].

We define the age of a derived cell as the number of telomere shortening divisions it has undergone since it transferred from the repopulating pool. The relation between the average telomere length in the derived pool and the average age $\overline{i(t)}$ is

$$\overline{L(t)} = L_0 - \Delta \overline{i(t)}, \tag{1}$$

where L_0 is the initial telomere length, assumed identical for all repopulating cells. A division of a cell of age $i-1$ results in one less cell of age $i-1$ and two additional daughter cells at age i. This occurs at a rate of M per time per cell. Therefore the change over time in the number of cells of age i, $N(i,t)$, is

$$\frac{dN(i,t)}{dt} = 2MN(i-1,t) - (M+D)N(i,t), \quad i > 0,$$

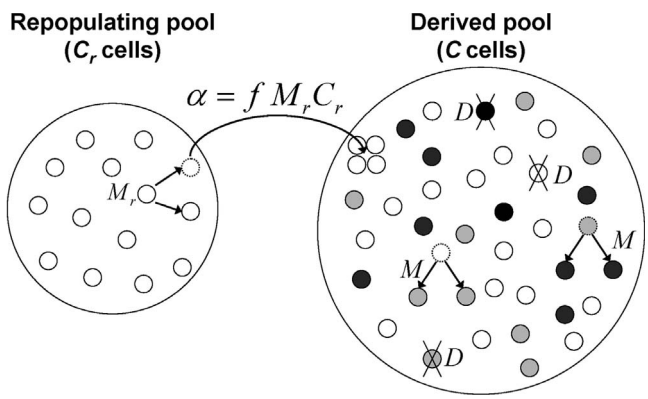

FIG. 1. Population mixture model. Circle shades denote telomere length, or number of divisions in the derived pool (light colors, low number of divisions; dark colors, high number of divisions). Dotted line cells will not be present in the next time point.

*Corresponding authors.

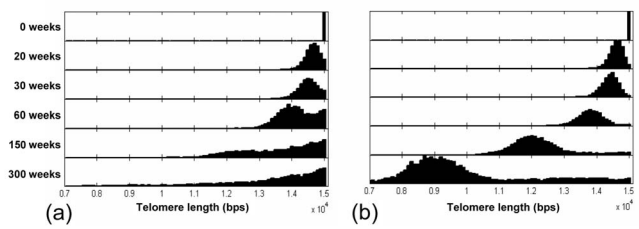

FIG. 2. Distribution of telomere lengths. Each row represents the distribution at different times. $M=0.1$/week, $C=10\,000$ cells. (a) $\alpha=130$ cells/week (half steady state is reached after 53 weeks). (b) Reduced repopulation rate, $\alpha=13$ cells/week (half steady state reached after 533 weeks).

$$\frac{dN(0,t)}{dt} = \alpha - (M+D)N(0,t), \quad i=0, \tag{2}$$

where α is the influx of cells of age 0 from the repopulating pool. Assuming that the total number of derived cells $C=\Sigma_{i=0}^{\infty}N(i,t)$ is constant (we relax this assumption below) and using Eq. (2) we obtain

$$\frac{dC}{dt} = 0 = \frac{d}{dt}\sum_{i=0}^{\infty} N(i,t) = \alpha - (D-M)C \Rightarrow D = M + \alpha', \tag{3}$$

where $\alpha'=\alpha/C$. Thus cell death in the derived pool is balanced by cell division in the derived pool and by an influx of repopulating cells. The master equation [17] for the distribution of cells at age i and time t, $P(i,t)=N(i,t)/C$, is

$$\frac{dP(i,t)}{dt} = 2MP(i-1,t) - (M+D)P(i,t), \quad i>0,$$

$$\frac{dP(i,t)}{dt} = \alpha' - (M+D)P(i,t), \quad i=0. \tag{4}$$

The dynamics of telomere shortening in the derived pool gives rise to a distribution of telomere lengths which changes with time (Fig. 2). Using the generating function [18–20] $F(x,t)=\Sigma_{i=0}^{\infty}P(i,t)x^i$ and Eq. (4) yields

$$\begin{aligned}\frac{\partial F(x,t)}{\partial t} &= \sum_{i=0}^{\infty}\frac{dP(i,t)}{dt}x^i \\ &= \alpha' - (M+D)P(0,t) \\ &\quad + 2M\sum_{i=1}^{\infty}P(i-1,t)x^i - (M+D)\sum_{i=1}^{\infty}P(i,t)x^i \\ &= \alpha' - (M+D)\sum_{i=0}^{\infty}P(i,t)x^i + 2Mx\sum_{i=0}^{\infty}P(i,t)x^i \\ &= \alpha' + [2Mx - (D+M)]F(x,t). \end{aligned} \tag{5}$$

Differentiating (5) with respect to x, substituting $x=1$, and using $\overline{i(t)} = \partial F(x,t)/\partial x|_{x=1}$ and $F(1,t)=1$ yields

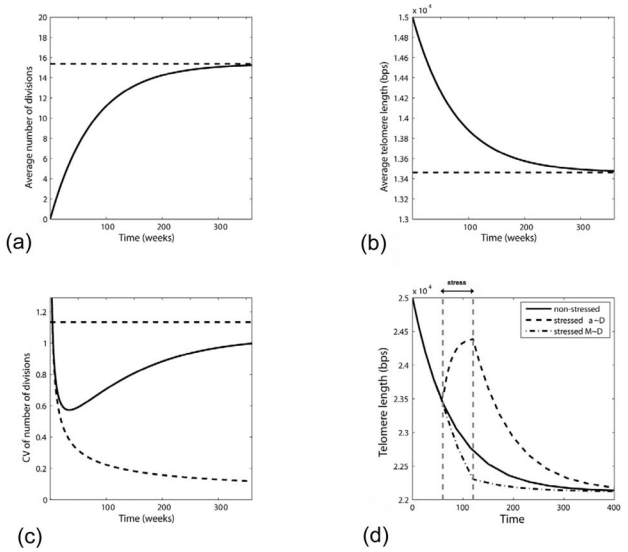

FIG. 3. Population mixture model predicts an exponential decline in average telomere length with time. (a) The average number of divisions of derived cells (cell age) increases nonlinearly with time. (b) Average telomere length decreases exponentially with time. (c) The coefficient of variance of the number of divisions of derived cells decreases first and then approaches a steady state exceeding 1. Solid line, theoretical cv; decreasing dashed line, short-time Poisson limit. (d) Different behaviors of telomere dynamics in response to stress. The death rate D was increased by 25% between time points 60 and 120. The solid curve shows the dynamics without perturbation, the dashed curve shows compensation through an increased repopulation rate ($\alpha' \sim D$), and the dash-dotted curve shows compensation through an increased derived cell division rate ($M \sim D$). Curves obtained by analytical solution of Eq. (7) with the parameters of Fig. 2(a).

$$\frac{d\overline{i(t)}}{dt} = \frac{\partial}{\partial x}\frac{\partial F(x,t)}{\partial t}\bigg|_{x=1} = 2M + (M-D)\overline{i(t)}, \tag{6}$$

with the solution [Fig. 3(a)]

$$\overline{i(t)} = \frac{2M}{D-M}(1-e^{-(D-M)t}) = \frac{2M}{\alpha'}(1-e^{-\alpha' t}), \tag{7}$$

where we have used Eq. (3)—namely, that $D-M=\alpha'$

Using Eqs. (1) and (7) the average telomere length is

$$\overline{L(t)} = L_0 - \frac{2M\Delta}{\alpha'}(1-e^{-\alpha' t}). \tag{8}$$

Thus the average telomere length decreases exponentially with a typical half time of $\tau_{1/2}=\ln(2)/\alpha'$ toward a steady-state level of $L_0-2M\Delta/\alpha'$ [Fig. 3(b)]. At the limit of $T \ll \tau_{1/2}$, where T is the relevant time of observation—e.g., the organism life span—Eq. (8) reduces to a linear decrease in average telomere length, $\overline{L(t)}=L_0-2M\Delta t$. This limit represents a single pool of cells, such as in tissue culture.

The distribution variance $v(t)$ can be obtained by differentiating Eq. (5) twice with respect to x and setting $x=1$:

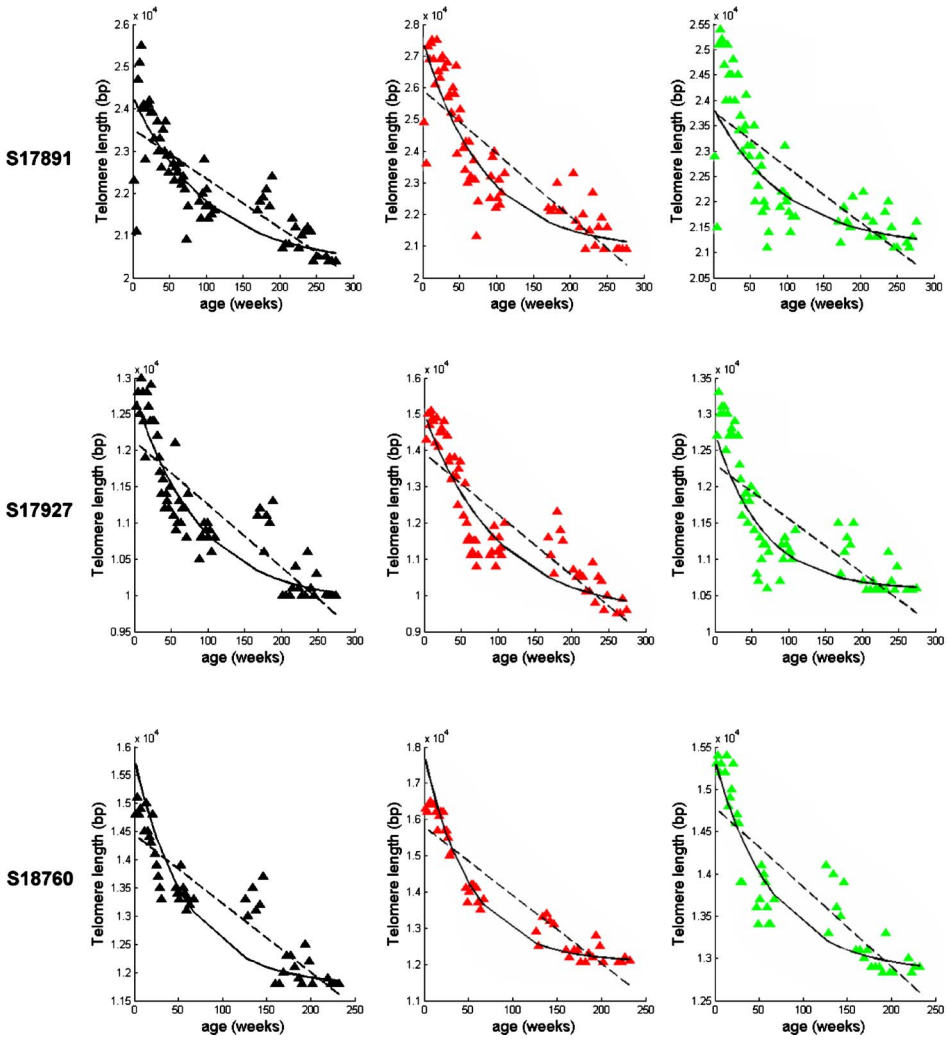

FIG. 4. (Color online) Exponential decrease in telomere lengths with age fits experimental data. Telomere length data for granulocytes (left, black), T cells (middle, red), and B cells (right, green) of three baboons were taken from [7]. Solid curves, model exponential fit. Dashed curves, linear fit. Except for granulocytes in S18760 the exponential fit provided a substantially better fit to the data (median reduction of 37% in least-squares error). See Table I for the parameters used.

$$v(t) = \frac{2M}{\alpha'}(1 - e^{-\alpha' t}) + \frac{4M^2}{\alpha'^2}(1 - e^{-2\alpha' t}) - \frac{8M^2 t}{\alpha'} e^{-\alpha' t}. \quad (9)$$

At short times after birth the coefficient of variance $(\mathrm{cv} = \sqrt{v}/\langle i(t)\rangle)$ behaves similarly to that of a Poisson distribution $(\mathrm{cv} = 1/\sqrt{i(t)}$. At later times the distribution width increases to approach $\sqrt{1 + \alpha'/2M}$ [Fig. 3(c)].

Using Eq. (5), the steady-state value of F is $F_{st} = \alpha'/(M + D - 2Mx)$; thus, the steady-state distribution is geometric with parameter $\alpha'/(M+D)$:

$$\begin{aligned} p(i)_{st} &= \frac{1}{i!}\frac{\partial^i F_{st}}{\partial x^i}\bigg|_{x=0} \\ &= \frac{\alpha'}{(M+D)}\left(\frac{2M}{M+D}\right)^i \\ &= \frac{\alpha'}{(M+D)}\left(1 - \frac{\alpha'}{(M+D)}\right)^i, \end{aligned} \quad (10)$$

while as at the steady state the distribution is highly skewed [Fig. 2(a)], at earlier times when $\alpha' \ll 1/T$, where T is the relevant observation time, the distribution is much more narrow [Fig. 2(b)], as previously observed in cultured cells [21].

To validate the model prediction of an exponential decrease in average telomere length with time, we used a published database of longitudinal leukocyte telomere length measurements in baboons at different ages [7]. We find that the exponential model fits the observed data much better than a linear decline in telomere length with age (Fig. 4). The median least-squares error of the exponential fit was 63% of that for the linear fit. The typical half time $(ln(2)/\alpha')$ of telomere reduction is approximately 50 weeks. Assuming a telomere decrease of 120 BPs per division [22] the fit for M predicts a division once every 5 weeks for granulocytes, once every 3 weeks for T cells, and once every 8 weeks for B cells (Table I).

Our model yields the same analytical solution if we assume that the number of cells increases exponentially with a

TABLE I. Parameter fits for the baboon data. Numbers in parentheses are standard errors in the last digit.

	α' (1/week)	$M\Delta$ (BP/week)
Granulocytes	0.013(2)	23(5)
T cells	0.014(3)	41(8)
B cells	0.013(2)	16(1)

constant rate $\gamma \equiv \frac{1}{C}\frac{dC}{dt}$ in both pools rather than being constant, as observed in childhood [23]. The equations for the distribution moments and steady state remain the same with D replaced by $D+\gamma$.

In cases of increased cell death D due to physiological perturbations, compensation can occur either by increasing M, yielding a more rapid decrease in average telomere length [24], or in α, yielding an increase in the average telomere length [Fig. 3(d)]. The latter mechanism may account for the surprising findings of telomere elongation in T cells of HIV patients [25,26] and in some patients following bone marrow transplantation [27,28]. After removal of stress the model predicts a return to the original steady state, $L_0 - 2M\Delta/\alpha'$.

The present model can be readily generalized to address more complex aspects of telomere dynamics such as regulation of the telomere length per cell division by telomerase, possible regulation of cell turn-over rates, the accumulation of senescent cells once telomere length crosses a critical threshold and the population dynamics of the repopulating pool. This, however, is beyond the scope of the present work.

In summary, we presented a model which explains how linear telomere dynamics at the single-cell level can give rise to exponential dynamics at the population level. The model assumes the existence of a repopulating pool of cells with telomeres of constant length and a derived pool of cells with telomere length decreasing linearly with the number of divisions. The model fits available longitudinal data, predicts a wide distribution of telomere lengths *in vivo*, and explains cases in which average telomere length increases following stress. The model facilitates inferring the existence of stem-cell populations and estimating implicit population parameters, such as division and repopulation rates. It will be interesting to apply the present model to human longitudinal data of telomere length and to extend the approach to the analysis of other dynamic biological attributes of cell populations.

We thank Peter Lansdorp for the baboon telomere length data and Eran Segal, Nir Friedman, Yair Shokef, and Tomer Kalisky for useful discussions. We gratefully acknowledge the support of Research Grant No. 5210 from the Ministry of Health, State of Israel.

[1] C. B. Harley, A. B. Futcher, and C. W. Greider, Nature (London) **345**, 458 (1990).
[2] N. E. Sharpless and R. A. DePinho, Nat. Rev. Mol. Cell Biol. **8**, 703 (2007).
[3] N. P. Weng *et al.*, Proc. Natl. Acad. Sci. U.S.A. **92**, 11091 (1995).
[4] H. Vaziri *et al.*, Proc. Natl. Acad. Sci. U.S.A. **91**, 9857 (1994).
[5] R. W. Frenck, Jr., E. H. Blackburn, and K. M. Shannon, Proc. Natl. Acad. Sci. U.S.A. **95**, 5607 (1998).
[6] H. Iwama *et al.*, Hum. Genet. **102**, 397 (1998).
[7] G. M. Baerlocher *et al.*, Aging Cell **6**, 121 (2007).
[8] N. Rufer *et al.*, J. Exp. Med. **190**, 157 (1999).
[9] S. L. Zeichner *et al.*, Blood **93**, 2824 (1999).
[10] I. A. Sidorov, D. Gee, and D. S. Dimitrov, J. Theor. Biol. **226**, 169 (2004).
[11] B. E. Shepherd *et al.*, Exp. Hematol. **32**, 1040 (2004).
[12] M. B. Bowie *et al.*, J. Clin. Invest. **116**, 2808 (2006).
[13] R. J. De Boer and A. J. Noest, J. Immunol. **160**, 5832 (1998).
[14] T. H. Brummendorf and S. Balabanov, Leukemia **20**, 1706 (2006).
[15] T. Antal *et al.*, J. Theor. Biol. **248**, 411 (2007).
[16] M. Garcia-Escarp *et al.*, Cell Tissue Res. **319**, 405 (2005).
[17] N. Friedman, L. Cai, and X. S. Xie, Phys. Rev. Lett. **97**, 168302 (2006).
[18] O. G. Berg, J. Theor. Biol. **71**, 587 (1978).
[19] J. Peccoud and B. Ycart, Theor Popul. Biol. **48**, 222(1995).
[20] M. Thattai and A. van Oudenaarden, Proc. Natl. Acad. Sci. U.S.A. **98**, 8614 (2001).
[21] P. M. Lansdorp *et al.*, Hum. Mol. Genet. **5**, 685 (1996).
[22] H. Vaziri *et al.*, Am. J. Hum. Genet. **52**, 661 (1993).
[23] S. M. Lewis, B. J. Bain, and I. Bates, *Dacie and Lewis Practical Haematology* (Churchill Livingstone, Philadelphia, 2006).
[24] S. Demissie *et al.*, Aging Cell **5**, 325 (2006).
[25] K. C. Wolthers *et al.*, Blood **93**, 1011 (1999).
[26] L. D. Palmer *et al.*, J. Exp. Med. **185**, 1381 (1997).
[27] N. Rufer *et al.*, Blood **97**, 575 (2001).
[28] Y. H. Li *et al.*, Bone Marrow Transplant **30**, 475 (2002).